Widespread coastal upwelling along the Eastern Paleo-Tethys Margin (South China) during the Middle Permian (Guadalupian): implications for organic matter accumulation

Bolin Zhang[a], Suping Yao[a], Paul B. Wignall[b], Wenxuan Hu[a], Hai Ding[c], Biao Liu[a], Yongle Ren[a]

[a] *MOE Key Laboratory of Surficial Geochemistry, School of Earth Sciences and Engineering, Nanjing University, Nanjing 210023, China*

[b] *School of Earth and Environment, University of Leeds, Leeds LS2 9JT, UK*

[c] *Exploration Research Institute, Anhui Provincial Bureau of Coal Geology, Hefei 230088, China*

Abstract: Guadalupian organic-rich depositions within the eastern Paleo-Tethys Margin have been attributed to coastal upwelling, but the idea has not been tested. Here, a suite of geochemical proxies from the Gufeng Formation of the Lower Yangtze region (South China) are used to investigate the formation mechanisms of organic matter accumulation. A high organic carbon content and similar enrichments of bio/redox-sensitive trace metals show strong similarities to the geochemical characteristics of modern upwelling sediments. The use of high Cd/Mo ratios and low Co x Mn values characteristic of modern upwelling settings (Sweere et al. 2016) is replicated in the Gufeng strata implying that Lower Yangtze area was dominated by persistent upwelling that become less intense (seasonal?) later in the Guadalupian. Application of these new geochemical proxies shows that the characteristics of modern upwelling systems, such as the formation of an intense oxygen minimum zone (OMZ), can be confirmed in the ancient. Calculation estimates show that primary productivity was sustained at moderate to high levels and was at comparable levels to those of the modern Peru upwelling system. OMZ-related anoxic conditions (with transient euxinic episodes) dominated permanently during the deposition of the Gufeng Formation and then

became more intense conditions (euxinia) later in the Guadalupian. The radiolarian chert/siliceous mudstone rhythms that coincide with fluctuations in major elements, organic carbon, total sulphur and trace metal concentrations may reflect dilution by biogenic silica. Chert Zr/Al ratios are also higher than in mudstone suggesting the cherts may record more winnowed deposition at the margin of an ancient OMZ compared with a location within the OMZ for the mudstone. The organic matter accumulation of the Middle Permian Gufeng Formation may be mainly controlled by the upwelling-driven primary productivity and also influenced by the changes of anoxic/euxinic conditions and the dilution of biogenic silica.

Keywords: geochemical proxies, high productivity, marine anoxia, trace metals, oxygen minimum zone

1. Introduction

The Guadalupian interval saw the deposition of some exceptionally organic-rich sediments, which have been associated with vigorous thermohaline circulation and upwelling of nutrient-rich cold waters (Murchey and Jones, 1992; Beauchamp and Baud, 2002). In South China these conditions are manifest as black chert-mudstone rhythms (i.e., Gufeng Formation, e.g., Feng et al, 1993; Kametaka et al, 2005; Yao et al., 2015; Wu et al., 2015), and they have been attributed to multiple, interacting processes of upwelling and river runoff under the control of Milankovitch-scale orbital forcings (Yao et al., 2015). One of the outstanding characteristics of the Gufeng Formation is its extremely high total organic carbon (TOC) content, which is often greater than 20 % (e.g., Liang et al., 2009; Saitoh et al., 2013; Du et al., 2015; Shi et al., 2016; Fig. 1b, c) making it one of the most important Palaeozoic petroleum source rocks in China (e.g., Xu, 1990; Liang et al., 2009; Du et al., 2015). However, there is little information available pertinent to the conditions

45 responsible for such organic-rich sediment deposition. An upwelling system has long been
46 considered a likely cause (Lv and Qu, 1989; Wang et al., 1997; Kametaka et al, 2005), but the
47 interpretation of the formation of these organic-rich sediment deposition is still unclear due to a
48 lack of diagnostic data to test such a scenario.

49 Generally, upwelling zones are not only areas of persistent high productivity in modern oceans
50 (e.g., the Peru Margin, Böning et al., 2004) but they are also considered important depositional
51 settings for ancient source rocks (Demaison and Moore, 1980; Parrish and Curtis, 1982; Parrish,
52 1982). Although it is easy to predict the location of ancient upwelling zones based on the their
53 palaeogeographic location (i.e., along the west coasts of continents; Parrish and Curtis, 1982;
54 Parrish, 1982) and lithologic characteristics (abundant phosphate, silica, and organic-rich
55 sediments; Lv and Qu, 1989; Wang et al., 1997; Kametaka et al, 2005), it is still difficult to
56 conclusively demonstrate that such sediments formed as upwelling deposits. Diagnostic
57 geochemical evidence is needed demonstrate the development of these ancient upwelling systems.

58 Different oceanographic and sedimentological factors, such as surface primary productivity
59 (e.g., Caplan and Bustin, 1999; Pedersen and Calvert, 1990; Tyson, 2005), bottom water redox
60 conditions (e.g., Canfield, 1989; Demaison and Moore, 1980) or dilution of terrestrial inputs (e.g.,
61 Ibach, 1982; Sageman et al., 2003), are generally considered the primary mechanisms for
62 contributing to the accumulation of organic-rich sediments. In addition, high productivity increases
63 the sinking flux of organic matter, thus favouring reducing conditions at depth, and intensified
64 anoxia results in greater P recycling, enhancing marine productivity in surface waters (Wignall,
65 1994; Algeo and Ingall, 2007). To better understand the effects of enhanced anoxia and increased
66 productivity on organic matter accumulation in the Gufeng Formation, a comprehensive

67 geochemical study has been carried out.

68 In this study, we use a series of geochemical proxy data, including total organic carbon (TOC),
69 total sulfur (TS), and major and trace element concentrations of the Middle Permian strata of the
70 Hexian core from the Lower Yangtze area to analyse an ancient upwelling system, reconstruct
71 palaeoenvironments and improve our understanding of the controlling factors of organic matter
72 accumulation. Changes in this sedimentary environment, including upwelling-driven primary
73 productivity, OMZ-related anoxic conditions and controls on organic enrichment are further
74 discussed to evaluate their role in organic matter accumulation.

75 ## 2. Geologic setting

76 The South China block was situated in the equatorial eastern margin of the Paleo-Tethys
77 Ocean and likely subject to prevailing northwest trade winds (Enkin et al., 1992; Wang and Jin,
78 2000; Fig. 1a). Intensive upwelling systems are thought to have stretched for hundreds of
79 kilometres along its margins during the Guadalupian (~272-262 Ma) based on the widespread
80 radiolarian chert and phosphate deposits on the northwest Yangtze Platform (Lv and Qu, 1989;
81 Wang et al., 1997; Kametaka et al, 2005). During this period, Gondwanan glaciation and cool
82 climates could have promoted a vigorous thermohaline circulation and intense upwelling
83 (Beauchamp and Baud, 2002). The widespread Gufeng Formation, a black, radiolarian chert-
84 mudstone succession characterized by extremely high TOC content (typically 4.3-16.8 %, with a
85 maximum of 27.6 %, Fig. 1b, c) was deposited along the northwest margin of the Yangtze Platform
86 (Fig. 1d). In the late Guadalupian, chert deposition was replaced by siliciclastic sedimentation
87 (Yinping Formation) possibly as a consequence of the cessation of the upwelling and/or global
88 regression (Bureau of Geology and Mineral Resources of Anhui Province, 1989; Yao et al., 2015).

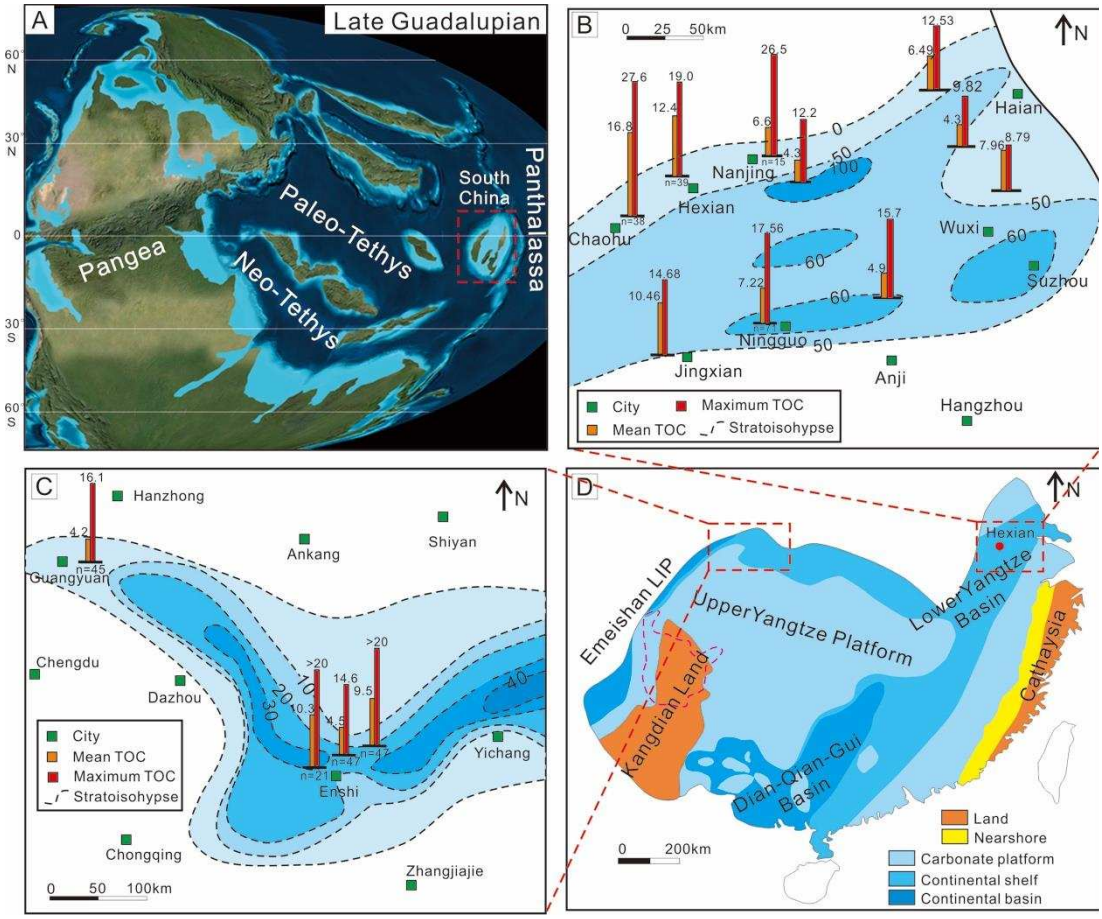

Fig. 1. (a) Late Guadalupian palaeogeography of the world. Base map from Ron Blakey (http://cpgeosystems.com). (b-c) Stratigraphic distribution and TOC characteristic of the Guadalupian organic-rich sediments in the Lower and Upper Yangtze area (modified from Liang et al., 2009; Saitoh et al., 2013; Shi et al., 2016; Wu et al., 2015). (d) Late Guadalupian palaeogeographic reconstruction of South China (modified from Yao et al., 2015).

Permian formations of the Lower Yangtze area are subdivided into the Qixia, Gufeng, Yinping, Longtan, and Dalong Formations in ascending order (Fig. 2). The Middle Permian strata are mainly composed of the Gufeng Formation and Yinping Formation (Fig. 2). In this study, we have principally focussed on the Gufeng Formation of the Hexian area, which is composed of two lithostratigraphic units (Fig. 2): a Lower chert-mudstone member (LCMM) and an Upper mudstone member (UMM). The LCMM is characterized by alternating beds of chert and siliceous mudstone, and the UMM consists only of black siliceous mudstone. The black chert contains microcrystalline quartz and/or chalcedonic quartz, organic particles and abundant well-preserved radiolarians (Fig. 2 a, b), whereas the black siliceous mudstone is mostly homogenous and lacks coarse terrigenous

clastic materials (Fig. 2c). Pyrite framboids are common accessory minerals in both units (Fig. 2d).

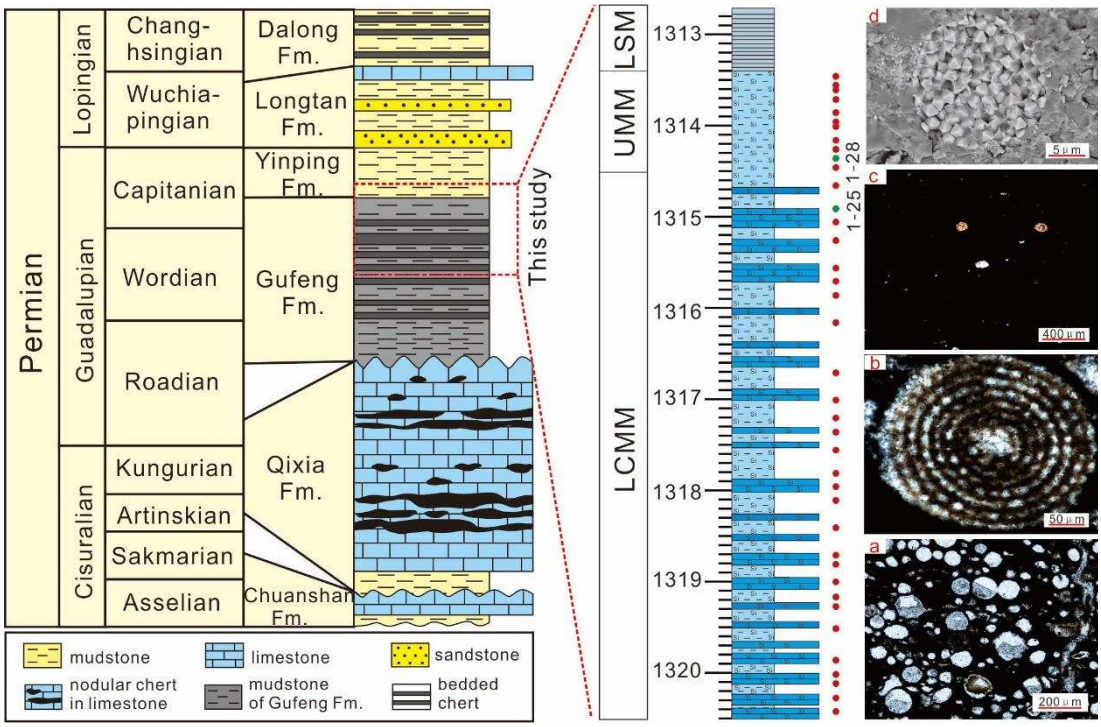

Fig. 2. Permian stratigraphy in the Lower Yangtze region (Yao et al., 2015) and lithologic strata of the Upper Gufeng Formation (LCMM and UMM) and the Lower Yinping Formation (LSM) in the Hexian area. (a) Black chert (sample 1-28) including abundant spheroidal radiolarians filled with chalcedonic quartz. (b) Radiolarian with a complete ring structure (sample 1-28). (c) Black siliceous mudstone with little radiolarians (sample 1-25). (d) Closed, small pyrite framboids of the siliceous mudstone (sample 1-25).

3. Samples and methods

A total of 39 samples, including black chert (n = 15) and siliceous mudstone (n = 24), were collected from the Upper Gufeng Formation of the Hexian core (Table 1, Fig 2) and pulverized to 200 mesh for geochemical analysis. Both TOC and TS content were measured by the Elementar® Vario MACRO CHNS elemental analyser at the Key Laboratory of Surficial Geochemistry of the Ministry of Education, Nanjing University. All samples were treated with 2 N HCl for 24 h to remove inorganic carbon, washed to neutral and dried for the final tests on the machine. Analytical precision was determined based on replicates of one reference material and two duplicate samples during each run (n = 10), and was typically better than 1 % for TOC and 5 % for TS.

The major element concentrations were determined by wavelength-dispersive X-ray

fluorescence spectrometry (XRF) technique on fused glass sheets. These were prepared by thoroughly mixing 1 g of the powdered samples with 11 g of a co-solvent ($Li_2B_4O_7$/$LiBO_2$/LiBr: 49.75 %/49.75 %/0.50 %) before they were melted in the platinum crucible using a THEOXD fully automatic electric melting furnace operating at 40 kV and 75 mA. Approximately 0.5 mg of the sample powders were weighed to burn in a muffle furnace at 1050 °C for 2 h. Loss on ignition (LOI) was calculated by the difference values of those burned samples. The sample analyses were carried out using an ARL9900 XRF with the geological standard (GBW-07103 and GBW-07105), yielding an analytical precision of ± 1 % for sample concentrations larger than 1 % and ± 10 % for sample concentrations less than 1 %.

The trace elements were measured using a Finnigan Element 2 mass spectrometer. Sample preparation was performed in a 100 ultra-clean laboratory using a brief experimental process that can be described as follows. ① Approximately 50 mg of each sample powder was weighed into PTFE inner cans and then dissolved with 1.5 mL of Concentrated (Conc.) HF before being evaporated to a nearly dry condition on a hotplate (130 °C); ② 1.5 mL of Conc. HF and 1 mL of Conc. HNO_3 were added to the cans, which were then re-sealed into steel jackets before being heated at 190 °C in an oven for 72 h; ③ after cooling, the jackets were opened and evaporated at 130 °C to a nearly dry condition on a hotplate, and the evaporation process was repeated twice while adding 1 mL of Conc. HNO_3; ④ the resultant salt was re-dissolved with 1 mL of Conc. HNO_3 and 2 mL of H_2O before it was again sealed and heated in the steel jacket in an oven at 190 °C for 12 h; and ⑤ after cooling, the final solution was transferred to a polyethylene bottle and diluted with 1 mL of a 500 ng/mL Rh internal standard solution to 50 mL for ICP-MS analysis. The analytical precision, determined by analyses of two international rock standards and two duplicate samples

during each run (n = 15), was typically better than 5%. Both major and trace elements were analysed at the State Key Laboratory for Mineral Deposits Research, Nanjing University.

Generally, enrichment factors (EFs) calculated as $X_{EF} = (X/Al)_{sample}/(X/Al)_{AUCC}$ (Brumsack, 2006; Tribovillard et al., 2006) were used to exclude the dilution effects and assess the authigenic fraction, in which X and Al are the weight concentrations of elements X and Al, respectively. The sample concentrations were normalized to the value of average upper continental crust (AUCC; McLennan, 2001). Detrital fraction ($TM_{detr} = Al_{sample} \times (TM/Al)_{AUCC}$, Brumsack, 2006; Tribovillard et al., 2006), biological fraction ($TM_{bio} = TOC_{sample} \times (TM/TOC)_{plankton}$, Little et al., 2015; Scott et al., 2017), and authigenic fraction ($TM_{auth} = TM_{bulk} - Al_{sample}(TM/Al)_{AUCC} - TOC_{sample} \times (TM/TOC)_{plankton}$, Scott et al., 2017) were used to identify the different fractions of trace metals (TMs) in sediments. The TM/TOC ratios for phytoplankton are from Ho et al., 2003; Ho, 2006; Moore et al., 2013; Little et al., 2015. It's noteworthy that the negative TM_{auth} values were interpreted as no substantial authigenic component in the trace elements and then were uniformly set to zero for convenient discussion.

4. Results

4.1 TOC and TS

The TOC and TS contents of the 39 samples are shown in Table S1. The residual TOC content of the Gufeng Formation is, on average, 12.4 % and ranges from 2.4 to 19.0 %. Systematic variations coincide with the lithological cycles (Fig. 3). Chert has a mean value of 8.5 %, whereas siliceous mudstone has a higher mean value of 14.9 %. It is noteworthy that both chert and siliceous mudstone in the Gufeng Formation have extremely high TOC enrichment values relative to that of average shale (Fig. 5 a). The TS contents also varied systematically throughout the profile (Fig. 3). Chert has a relatively low TS content (mean 1.3 %), whereas siliceous mudstone has a higher TS

content (mean 3.0 %). Almost all chert samples contain <2 % TS and <12 % TOC, whereas most siliceous mudstone samples contain >2 % TS and >12 % TOC. In addition, the UMM has relatively higher TOC and TS contents (mean 16.5 % and 3.6 %, respectively) than the LCMM (mean 11 % and 2.1 %, respectively).

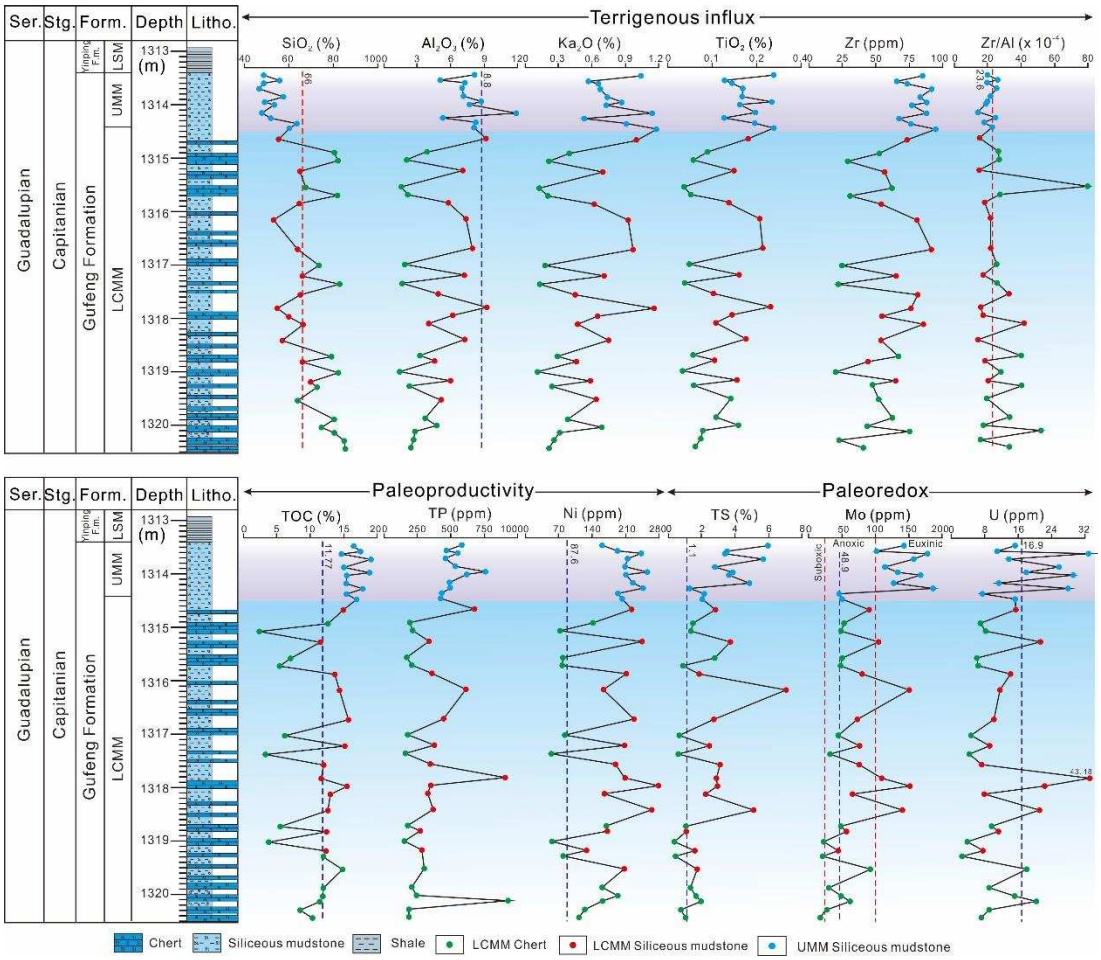

Fig. 3. Stratigraphic distributions of Hexian core for SiO_2, Al_2O_3, Ka_2O, TiO_2, Zr, Zr/Al, TOC, P, Ni, TS, Mo and U. The red dotted lines indicate the values of average upper continental crust (AUCC, McLennan, 2001), and the blue dotted line indicate the values of Peruvian sediments (Böning et al., 2004). Abbreviations: Ser. = Series, Stg. = Stage, Form. = Formation, Litho. =Lithology.

4.2 Major elements

The major elemental compositions of the 39 samples are listed in Table S2. The Gufeng Formation is enriched in SiO_2 (mean 65.6 %) relative to Al_2O_3 (mean 5.4 %) and CaO (mean 4.0 %), which are considered the major components of clay-rich mudstone (e.g., Ross and Bustin, 2009). The distinct enrichment in SiO_2 compared to Al_2O_3 is due to the abundant radiolarian content

(which is often converted into microcrystalline quartz and/or chalcedonic quartz during diagenesis). Clear negative correlations (R^2 = 0.68) are observed between the abundance of SiO_2 and Al_2O_3 for individual chert and mudstone beds (Fig. 4a), indicating the dilution of radiolarian remains by terrigenous detrital inputs (or vice versa). The Al_2O_3 in the chert and siliceous mudstone of the LCMM also exhibits a negative correlation with CaO (Fig. 4b), which suggest that Ca has a distinct origin, such as a biogenic source. The Gufeng Formation samples have low (<1%) TiO_2 and K_2O contents that fluctuate considerably. The Al_2O_3 shows a strong positive correlation with TiO_2 and K_2O (R^2 = 0.86 and 0.92, respectively), which suggests that Ti and K are associated with a detrital source linked to clay minerals (Fig. 4c, d). The Fe_2O_3 contents of the Gufeng Formation are relatively high (mean 3.0 %), but they are lower in the bottom of the LCMM, and they have a good correlation with TS (R^2 = 0.94, Fig. 4f). The chert and siliceous mudstones in the LCMM have relatively low P contents (mean 200 ppm and 435 ppm, respectively, Fig. 3), whereas the siliceous mudstones of the UMM have higher P contents (mean 528 ppm).

The enrichment factor is commonly used to estimate the enrichment degree of elements in sediments compared average upper continental crust. The major element enrichment factors of the Gufeng Formation are shown in Table S2 and Fig 5a. Both chert and siliceous mudstones have relatively high EF values for Ca, Si, P and Mg but relatively low EF values for K and Ti (Fig. 5a). The Fe content shows a slight enrichment in siliceous mudstone, but a slight depletion in chert (Fig. 5a). The enrichment of Ca, Si and P can be attributed to the biogenic sources, while the depletion of K and Ti suggest a low terrigenous input.

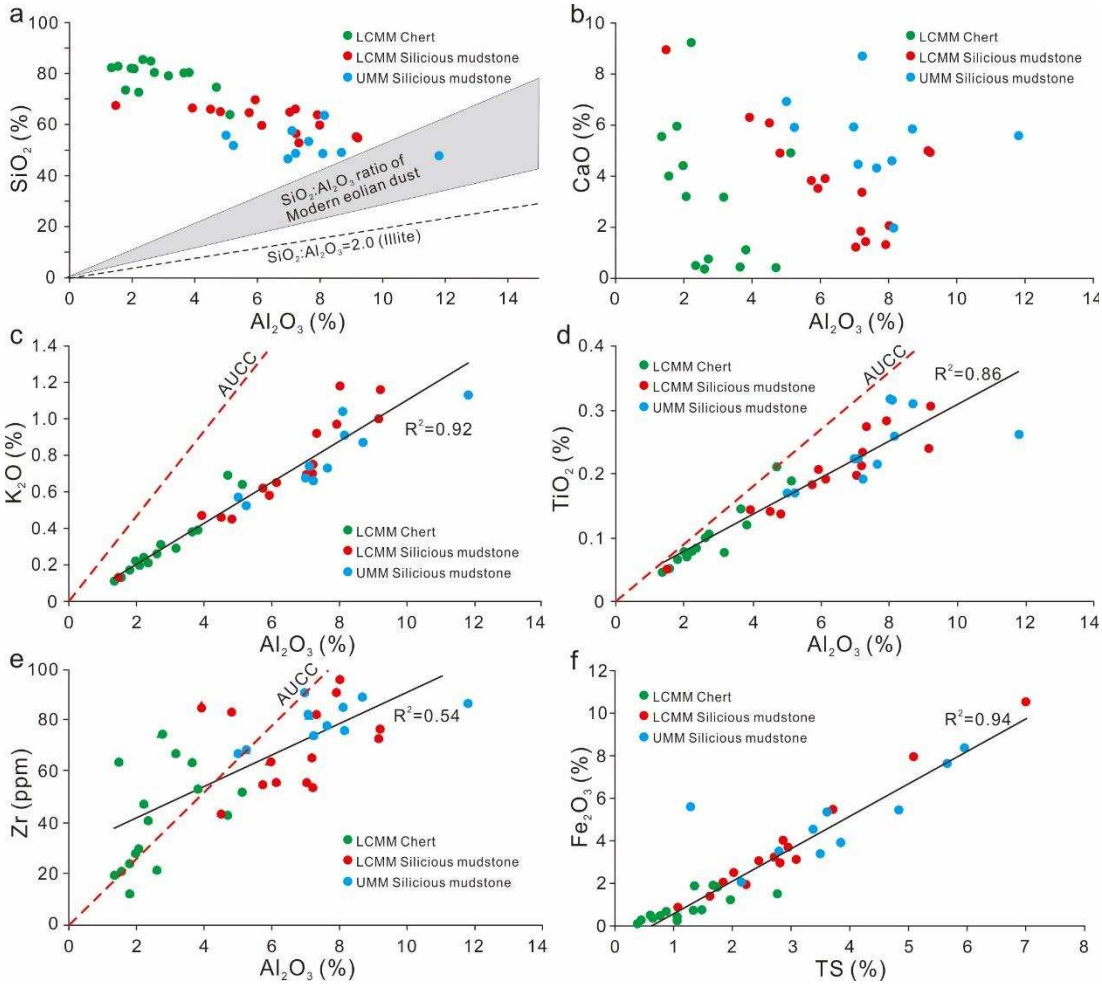

Fig. 4. (a) Crossplot of Al_2O_3 vs SiO_2 (cf. Ikeda et al., 2017) showing the ratio of analysed samples in this study are not in the range encountered for modern pelagic aeolian dust (grey shade, Lawrence and Neff, 2009). (b-f) Crossplots of Al_2O_3 vs CaO, Al_2O_3 vs K_2O, Al_2O_3 vs TiO_2, Al_2O_3 vs Zr, and TS vs Fe_2O_3. The red dotted lines indicate the values of average upper continental crust (AUCC, McLennan, 2001).

4.3 Trace elements

The analytical results for the trace elements content and relevant parameters are given in Table S3. Trace element concentrations in the Gufeng Formation fluctuate, with relatively low contents in chert and higher values in siliceous mudstone. The enrichment factors of most, large ion lithophile trace elements (e.g., Be, Ce, Cs, La, Pb and Rb) are relatively uniform in all lithotypes (Fig. 5b) due to their terrigenous origin, whereas Ba, which is derived from both detrital and biogenic origins and is recycled in a more reducing water columns, is relatively depleted in the mudstone. The enrichment factors of most, high-field-strength elements (Zr, Hf, Nb, Ga and Th),

which are attributed to aluminosilicate components and correlated with Al_2O_3,

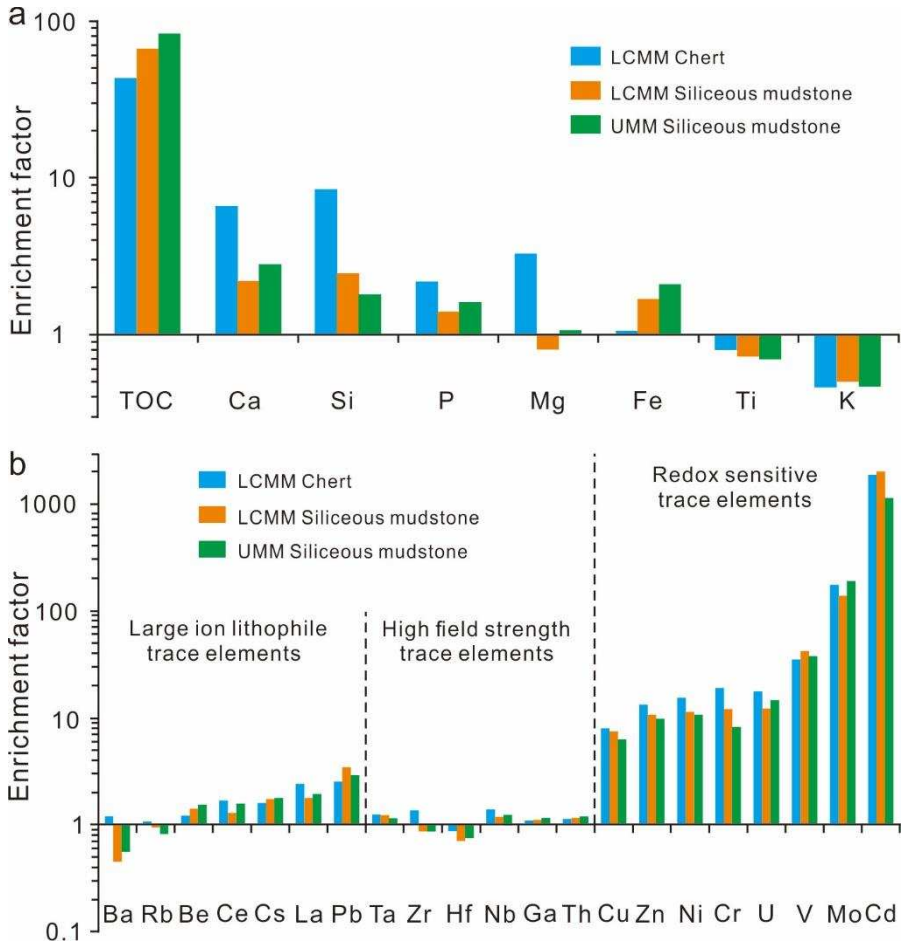

Fig. 5. Enrichment factors (EF) of TOC and major elements (a), and trace elements (b) in Gufeng chert-mudstone sequence compared to AUCC (McLennan, 2001). A horizontal line represents EF_{AUCC} = 1 to emphasize element enrichment or depletion.

also show relatively uniform values in all lithotypes, except for Ta (Fig. 5b). All lithologies of the Gufeng Formation are enriched in redox-sensitive trace elements (RSTEs, e.g. Cu, Zn, Cr, U, V, Mo and Cd; Fig. 5b), even when compared with other organic-rich sediments. The LCMM has high and fluctuating Ni values, whereas the UMM has relatively stable and higher Ni values (Fig. 3). The Mo and U have similar variations, with high contents in the Gufeng Formation and peaks in the lower LCMM and UMM (Fig. 3).

5. Discussion

5.1 Identifying sources and fractions of trace elements

Trace metals can be of detrital, biological and authigenic origin in the black shales (e.g., Scott et al., 2017), and distinguishing these components is crucial when interpreting the palaeoenvironmental setting. The dilution effect of detrital (e.g., aluminosilicates) and biological (e.g., biogenic silica) materials, is also known as the closed-sum effects (Rollison, 1993; Van der Weijden, 2002), and is a major factor when interpreting trace metal abundances. Accounting for these effects can be achieved by normalization of element concentrations to Al (e.g., Calvert and Pedersen, 1993; van der Weijden, 2002), a technique which assumes the Al is entirely of detrital origin, which is not without its pitfalls (van der Weijden, 2002; Tribovillard et al., 2006). To make results of the normalization procedure easier to interpret, here we calculated the detrital, biological and authigenic fractions (e.g., Tribovillard et al., 2006, Scott et al., 2017) to identify the main sources of trace elements in our samples.

The detrital contents of most TMs (e.g., Zn, Cr, U, V, Mo and Cd) in our samples are estimated to account for the small part (<~10%, Table S4, Fig. 6 and 7a, b, c). And values of these trace metals in phytoplankton (TM/TOC ratios, e.g., Ho et al., 2003; Moore et al., 2013; Little et al., 2015), which can be used as a rough estimate of the potential biogenic component (Scott et al., 2017), indicates that the biological fraction in sediments is small and can be ignored (Table S4, Fig. 6 and 7d, e, f). As shown in figure 6 and Table S4, the main part of these trace elements, except Mn and Co, resided in sediments is authigenic fraction, which may be mainly preserved as their sulphides (Fig. 7g, h, i) and very valuable when trying to interpret geochemical data. Thus we will use bulk concentrations of TMs for interpretation in the following discussion, due to the small detrital and biological

219 contribution of these TMs (e.g., Scott et al., 2017).

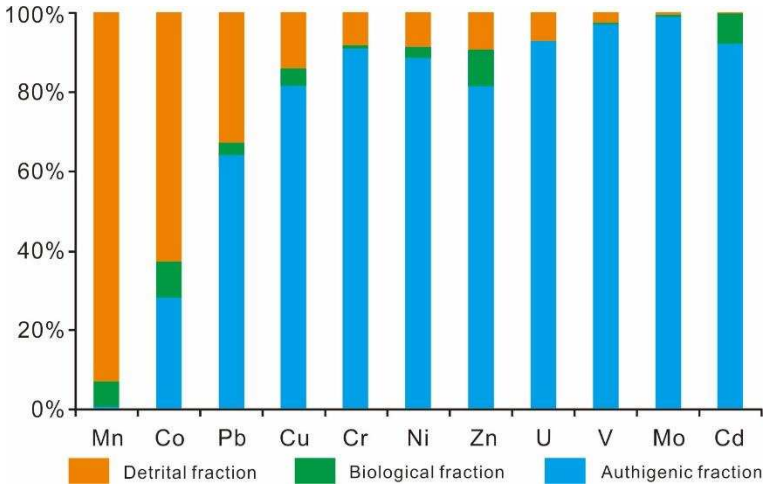

Fig. 6. Comparison of detrital, biological and authigenic fractions of trace metals in the Gufeng Formation.

220

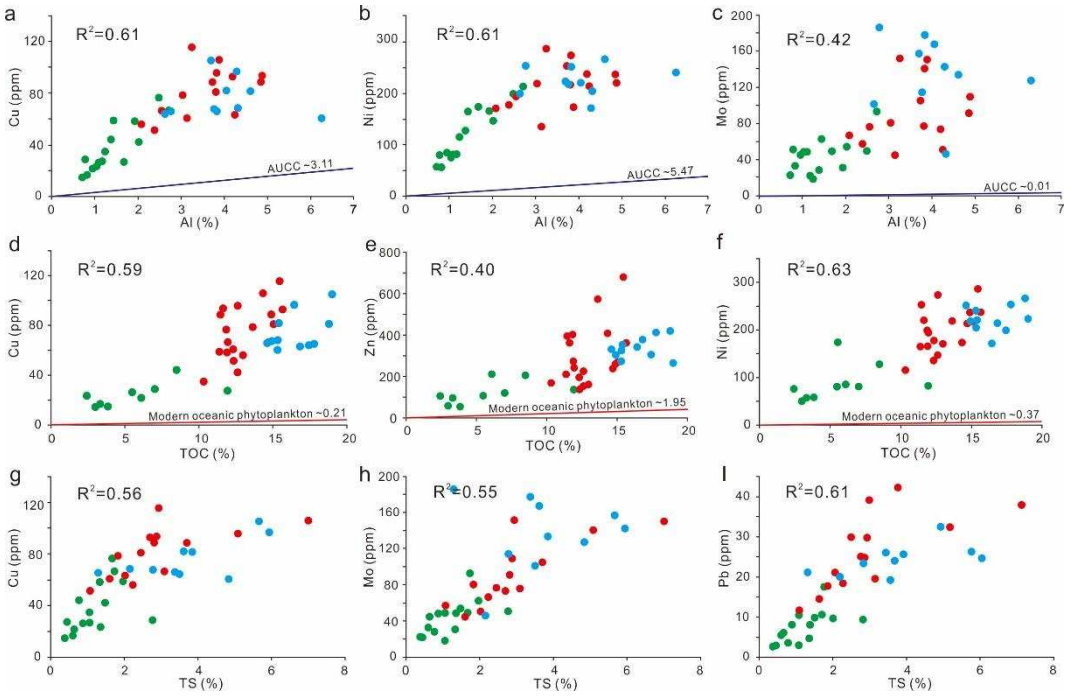

Fig. 7. Scatter plots of (a-c) Al vs. Cu, Ni, and Mo, (d-f) TOC vs. Cu, Zn, and Ni, (c) TS vs. Cu, Mo, and Pb. The blue lines indicate the values of average upper continental crust (McLennan, 2001), and the red lines indicate the values of Modern oceanic phytoplankton (Little et al., 2015). The legend is the same as figure 4.

221 ## 5.2 Geochemical evidence of coastal upwelling

222 Modern coastal upwelling settings (e.g., the Peru and Namibia margins) are characterized by

223 high primary production, high organic matter and trace metal accumulation and the formation of

224 an OMZ with intense sulfate reduction at its core (Böning et al., 2004, 2015; Brongersma-Sanders

et al., 1980; Robinson et al., 2002; Scholz et al., 2011). A suite of geochemical proxies, from these modern upwelling settings, can be used to identify ancient sediments formed under upwelling from other marine environments and help reconstruct palaeoenvironments.

5.2.1 High TOC contents

The highest accumulation rate of OM, indicated by corresponding sediment TOC content, can locally reach 27% on the Peru Margin and Namibian Shelf, is an important characteristic of modern upwelling settings (Brongersma-Sanders et al., 1980; Robinson et al., 2002; Böning et al., 2004, 2015; Scholz et al., 2011). The black chert-mudstone rhythmic sequence of the Gufeng Formation in the Hexian area has an extremely high TOC content, similar to those of the modern upwelling settings (Böning et al., 2004; Brongersma-Sanders et al., 1980; Robinson et al., 2002; Scholz et al., 2011). Values are higher than those found in modern euxinic environments (e.g., Black Sea and Cariaco Basin, Lyons and Berner, 1992; Lyons et al., 2003). Thus, the especially high TOC values (>20 %) along many sites on the northwest margin of South China (Fig. 1b, c), are considered particularly indicative of high OM accumulation and primary productivity of an ancient upwelling system, although the cherts are notably less enriched (Fig. 3, 5a). This is likely to reflect dilution of the biogenic silica although it may also reflect oscillation of the palaeo-OMZ with more radiolarian-rich sediments developed at the margins of the zone.

5.2.2 Bulk sedimentary composition

The chemistry of modern upwelling sediments is typically dominated by a mixture of lithogenic material, biogenic opal and biogenic carbonate (e.g., Böning et al., 2004, 2005). The similarity of the Gufeng Formation bulk sedimentary composition (except for P content) suggests comparable sediment sources (e.g., the Peruvian sediments, Fig. 8). Thus, the high enrichments of

247 Ca and Si suggest a biogenic origin due to high primary productivity, and the low enrichments of
248 other detrital proxies (e.g., Mg, K, Ti) indicate low inputs of terrigenous detritus in a deep water
249 setting far from shore. The lack of P enrichment in the Gufeng Formation may be the result of a
250 stronger remineralization in more reducing conditions than those eencountered on the modern
251 Peru margin (e.g., Ingall and Jahnke, 1997; Böning et al., 2004), which is further confirmed by the
252 higher TOC/TP ratios (mean 355) of the Gufeng Formation. Although some samples show major
253 excursions in SiO_2 due to higher amounts of radiolarian remains, most samples plot close to values
254 from modern upwelling settings (e.g., Gulf of California, Namibia, Peru), as shown in Figure 9.

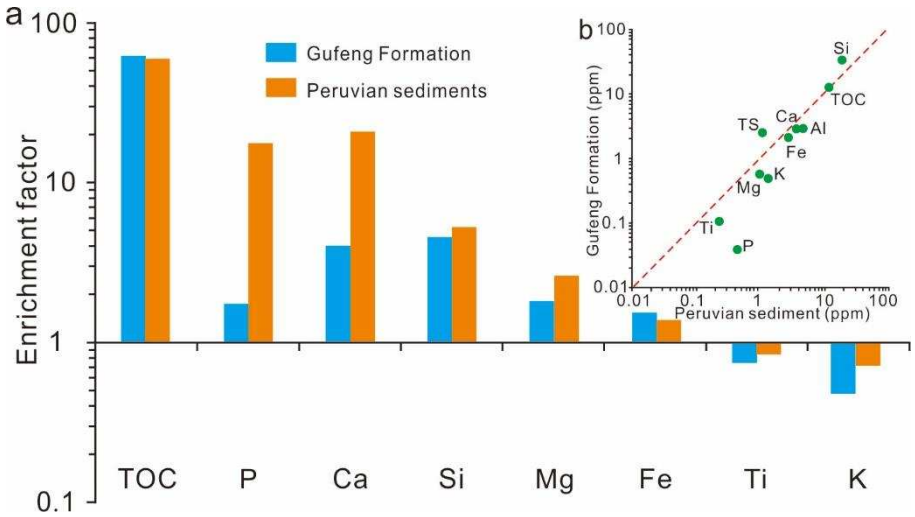

Fig. 8. (a) Enrichment factors (EFs) of TOC and major elements in Gufeng chert-mudstone sequence, in comparison to Peruvian sediments (Böning et al., 2004, 2009). (b) Crossplots of Peruvian sediments and Gufeng Formation with average values of their TOC, TS and major elements.

255

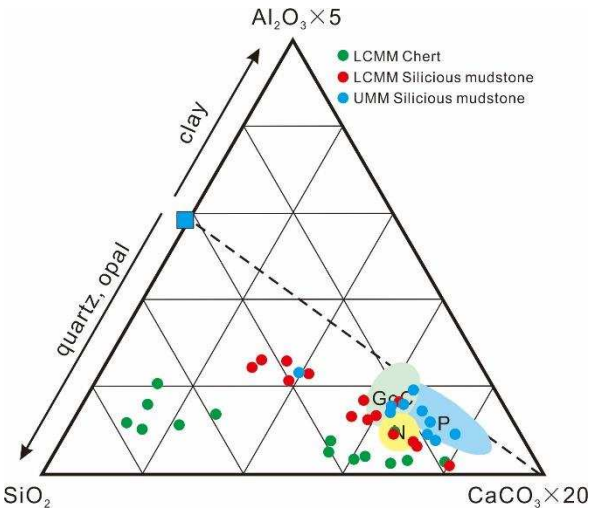

Fig. 9. Components of the Gufeng Formation in the system SiO_2-Al_2O_3 x 5-$CaCO_3$ x 20 (relative weight ratios) (modified from Böning et al., 2004). The square represents the data point for average shale (Wedepohl, 1991). GoC = Gulf of California, N = Namibia, P = Peru (Brumsack, 1989; Böning et al., 2004; Borchers et al., 2005).

5.2.3 Bio/redox-sensitive trace metal (TM) accumulation

Many modern upwelling sediments (e.g., the Gulf of California, Brumsack, 1989; Namibia Margin, Calvert and Price, 1983; Peru Margin, Böning et al., 2004; Chilean Margin, Böning et al., 2005, 2009) are characterized by significant enrichments of many trace metals (e.g., Cd, Cu, Cr, Ni, Mo, U, V, and Zn) due to high primary productivity and/or enhanced preservation under oxygen deficiency (Böning et al., 2004, 2009). The Gufeng Formation shows extremely high Cd and Mo contents, high Cu, Zn, Ni, Cr, U and V contents, slightly elevated Co and Pb, and depleted Mn (Fig. 5 and 10a). These bio/redox-sensitive TM enrichments are typical of those seen in upwelling settings (e.g., Böning et al., 2004, 2009), as confirmed by the strong correlation of TM concentrations of the Gufeng Formation with modern Peruvian upwelling sediments (Fig. 10b). The co-occurrence of extremely high Cd and Mo enrichments, in contrast to other TM in both the Gufeng Formation and modern upwelling sediments, is a further feature that distinguishes upwelling systems from marine environments where restricted conditions lead to anoxia (Sweere et al., 2016). Such enrichments are associated with the high primary productivity and reducing

condition of OMZs (e.g., Böning et al., 2004). The slightly higher overall enrichment of TM contents in the Gufeng Formation (Fig. 10a) may be due to factors such as the higher availability of metals in Permian seawater or a difference of terrigenous input. However, the significantly depleted Mn may be the result of its significant loss within the OMZ and/or the reducing sediments, and the slightly elevated Co may result from its fixation as a sulfide when sulfidic conditions prevail (Heggie and Lewis, 1984). Therefore, the significant bio/redox-sensitive TM enrichment in the Gufeng Formation suggests an upwelling setting characterised by high productivity and strongly reducing conditions.

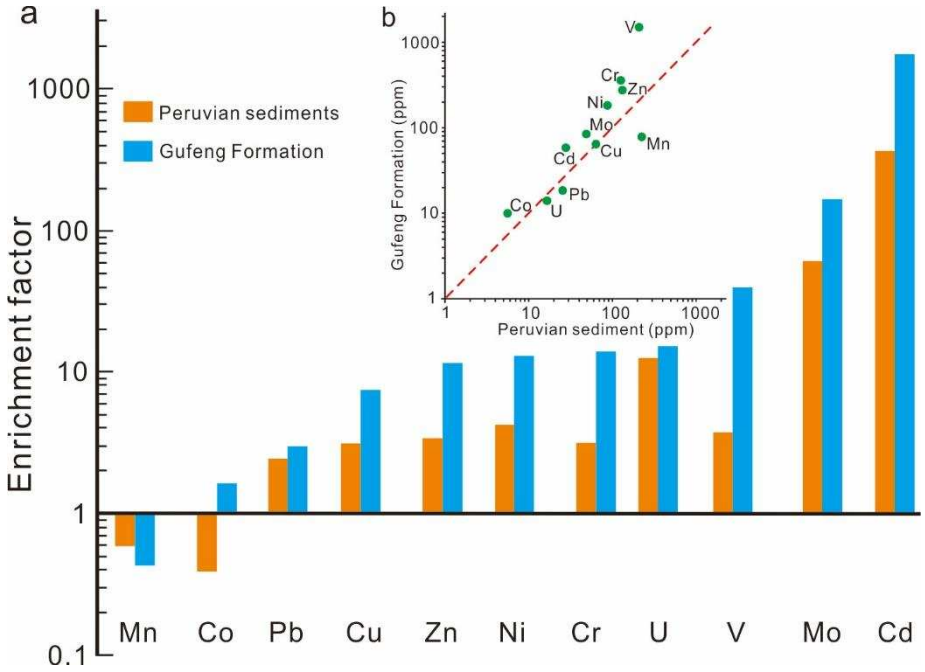

Fig. 10. (a) Enrichment factors of several bio/redox-sensitive TM for Gufeng samples in comparison to Peruvian sediments (Böning et al., 2004, 2009). (b) Crossplots of Peruvian sediments and Gufeng Formation with average values of these bio/redox-sensitive TM.

5.2.4 Cd/Mo ratio and Co x Mn value

Due to the significant depletion of Mn and Co and the exceptional enrichment of Cd and Mo in modern upwelling sediments (e.g., Peruvian Margin, Böning et al., 2004), the combined use of the Cd/Mo and Co x Mn proxy has been proposed as a valuable way to distinguish upwelling environments from other marine environments, especially restricted settings such as the modern

283 Black Sea (Sweere et al., 2016). High Cd/Mo ratios above 0.1 and low Co x Mn values below 0.4 or

284 low EF(Mn) x EF(Co) values below 0.5 are typical for sediments from coastal upwelling settings

285 (Sweere et al., 2016). Furthermore, those areas subject to persistent upwelling (e.g. Peruvian

286 Margin) having much higher Cd/Mo ratios and lower Co x Mn or low EF(Mn) x EF(Co) values than

287 those with only transient/seasonal upwelling (e.g. Gulf of California).

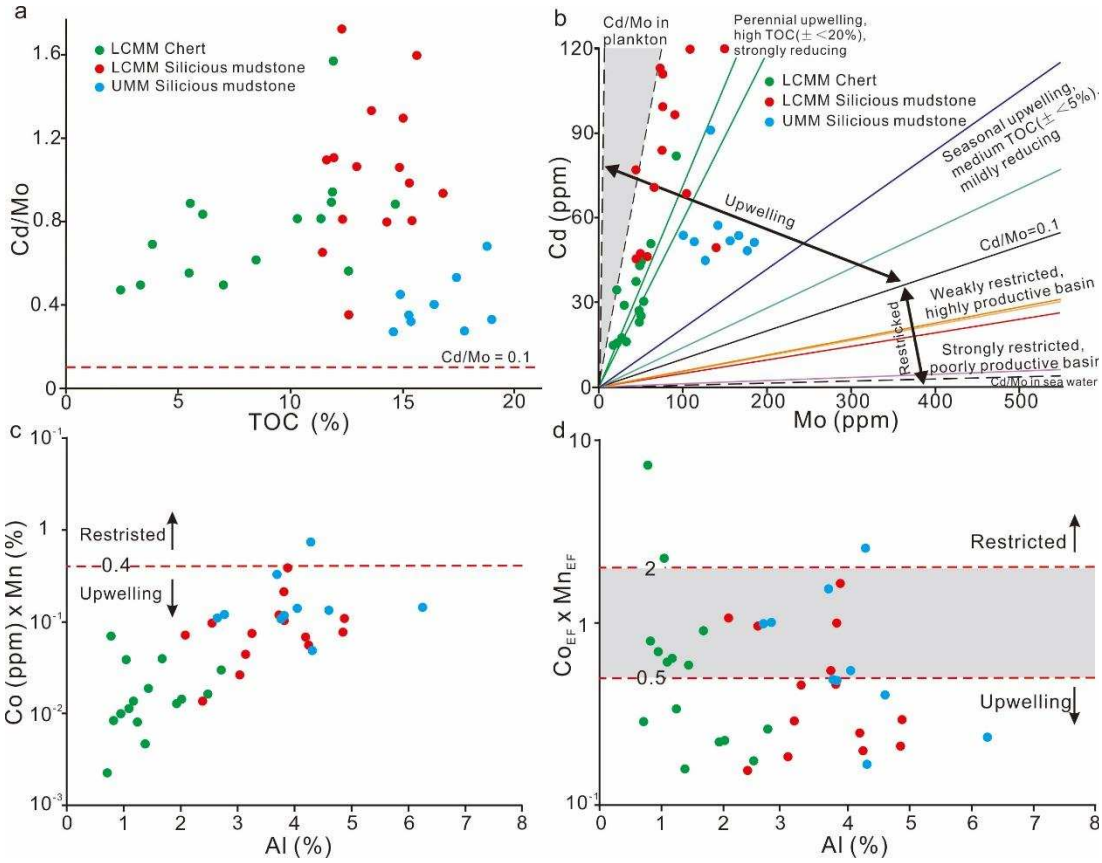

Fig. 11. (a) Cd/Mo ratios versus TOC content (%). (b) Mo versus Cd plot showing characteristic of upwelling setting. (c) Co x Mn versus Al. (d) Co_{EF} x Mn_{EF} versus Al. (inferred conditions based on modern settings, after Sweere et al., 2016).

288 The average Cd/Mo values of the Gufeng Formation is 0.79 suggests strong upwelling (Fig.

289 11a) as a result of a large flux of plankton-associated Cd to the sediment. This is confirmed by the

290 clear co-variation (R^2=0.58) between the Cd/Mo ratio and TOC content of the LCMM (Fig. 11b). The

291 presence of free H_2S resulting from sulfate reduction seems to be the key process for their

292 accumulation (Böning et al., 2004, 2009). In contrast, there is no correlation for both elements in

293 the UMM where increased Mo, but unchanged Cd contents, suggests a euxinic environment but
294 one only subject to seasonal upwelling (Fig. 11b).

295 The low Co x Mn values (below 0.4) and low EF(Mn) x EF(Co) values of the Gufeng samples
296 (Fig., 11c,d) is also distinctive and typical for modern sediments from continental margin upwelling
297 settings where the Mn (and probably also the Co) is lost to a "conveyor belt" process (current
298 transport of soluble Mn) (Sweere et al., 2016). In such a scenario, where there is weak authigenic
299 enrichment of these TMs, the Co and Mn are associated with detrital input only. The relatively
300 good correlation between Al and Co x Mn values in the Gufeng Formation is consistent with this
301 detrital scenario (Fig., 11c).

302 **5.2.5 P-Cd and Cd-Mo**

303 The strong association of Cd and P in modern oceans (Boyle et al., 1976; Bruland, 1983), and
304 phosphatic deposits (e.g., Baturin and Oreshkin, 1985; Nathan et al., 1997), indicates a significant
305 relationship between them in biodetritus and sediments (Böning et al., 2004). However, the
306 Peruvian Margin sediment has a unique characteristic with significantly enriched Cd but rather low
307 P contents, which results from the preferential loss of P relative to Cd in the reducing water column
308 or sediments (Böning et al., 2004). Furthermore, sediments within the OMZ have more enriched
309 Cd and relatively increased P compared to samples from the upper edge of the OMZ (Böning et al.,
310 2004). Similarly, exceptionally enriched Cd and Mo in sediments from the centre of the OMZ
311 compared to moderate enrichments from the zone's margins (Böning et al., 2004) could help
312 distinguish between different OMZ sites in the past.

313 The Gufeng Formation sediments are characterized by extremely enriched Cd and Mo with
314 rather low P contents, which are very similar to those of the Peruvian Margin. The strong

correlation of Cd and P (R^2 = 0.80) in the LCMM (Fig. 12a) suggests that this similar nutrient-like distribution in these ancient sediments with a high productivity supported by sufficient Cd inputs with efficient P cycling, whereas the good correlation for Mo and Cd (R^2 = 0.58) in the LCMM suggests similar mechanisms of preservation. With its increased P and Mo contents, and a stable Cd content the UMM (Fig. 12), may have had a more limited supply of Cd due to less persistent (seasonal?) upwelling. The distinct differences in the distribution and enrichment of these elements between chert and siliceous mudstone in the LCMM suggest that they may have developed in different OMZ sites resembling the modern Peruvian Margin. As shown in Figure 12, the chert mainly deposited in the upper edge OMZ whereas the siliceous mudstone deposited within OMZ. Alternatively, the dilution effect of radiolarian silica in the chert may be responsible for the depletion of TM concentrations.

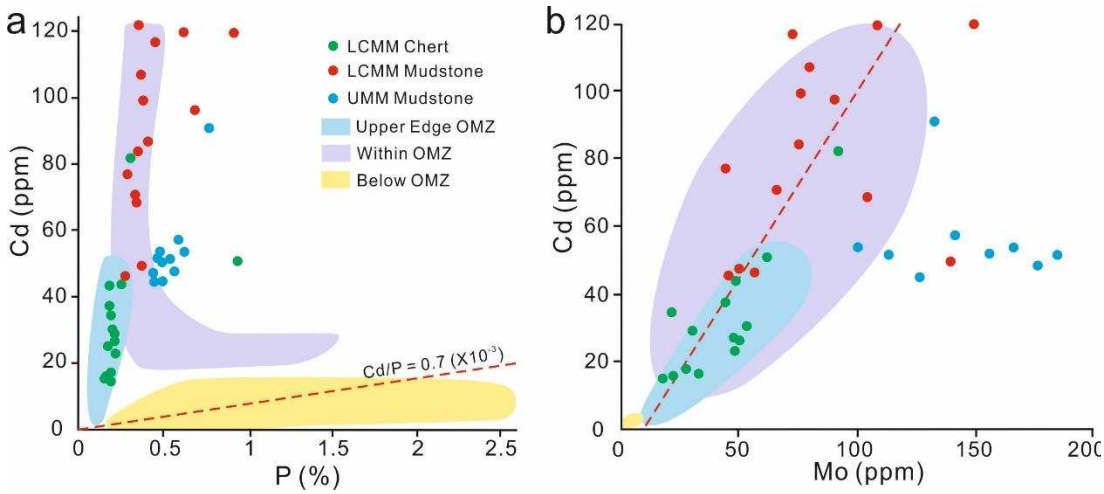

Fig. 12. Scatter plots of (a) P_{xs} vs. Cd, (b) Mo vs. Cd. (modified from Böning et al., 2004)

5.3 Reconstruction of this ancient upwelling environment

5.3.1 Upwelling-driven primary productivity

The metal Ni is used as a reliable indicator of organic sinking flux because it is only weakly associated with sulfur and manganese cycling in the water column and sediments (Böning et al., 2015), whilst other bio-sensitive elements (e.g., Cu, Cd and Zn) are rapidly removed during euxinia

as sulfides (Haraldsson and Westerlund, 1988; Morse and Luther, 1999). In addition, the strong correlation of Ni and original chlorophyll flux in modern oceans indicates a direct biochemical association of Ni with productivity, which further supports the idea that Ni can serve as a more robust indicator for productivity (Böning et al., 2015).

In this ancient upwelling setting, the significant linear relationship between Ni and TOC of the Gufeng Formation (R^2 = 0.63) supports the use of Ni as an indicator of productivity (Fig. 13). Peruvian OMZ sediments also record covariance of Ni and TOC indicating this is a distinct characteristic of upwelling systems. The Ni concentrations in the Gufeng Formation follow the stratal cyclicity with relatively low values in the chert but higher values in the siliceous mudstone (Fig. 3) probably due to dilution effects of the radiolarian flux in the cherts. In contrast, values are stable in the lithologically uniform UMM and closely comparable to values from Peru upwelling sediments although with higher Ni/TOC ratios (Fig. 13). Thus these systematic variations suggest that primary productivity was sustained at moderate to high levels.

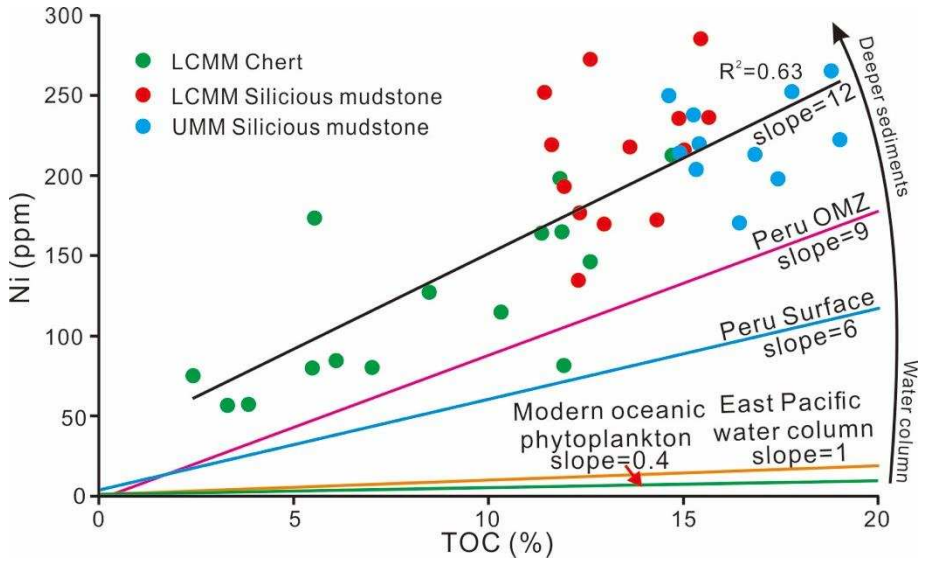

Fig. 13 Scatter plots of Ni vs TOC of Gufeng Formation (after Böning et al., 2015).

Both TOC and TP contents are commonly considered useful indicators of primary productivity (e.g., Schoepfer et al., 2015; Shen et al., 2015), and they too vary with the alternation of chert and

siliceous mudstone which again could be due to dilution effects (Fig. 3). Furthermore, primary productivity can be estimated using the empirical formula $PROD_{prim} = (10^{8.55} \times TOC \times LSR \times \rho)^{0.43}$, where LSR represents the consistent linear sedimentation rate (m Myr^{-1}) and ρ represents the sample bulk density (g cm^{-3}) (Schoepfer et al. 2015). Owing to the close distance (~50 km) and similar palaeogeographic environment (slope/basin) within the Chaohu area, we consider that the Hexian area has a consistent LSR with the Chaohu area of 4.8 m/Myr (Yao et al., 2015). For convenience, ρ was assumed to be 2.5 g cm^{-3} for all samples. The calculation gives estimated palaeo-productivity ranging from $2 – 4.9 \times 10^4$ mg cm^{-2} kyr^{-1} with an average of 4×10^4 mg cm^{-2} kyr^{-1}. These values are similar to those of modern upwelling environments (e.g., Chile-Peru coast, California Current and Benguela Current, $3.2 – 4 \times 10^4$ mg cm^{-2} kyr^{-1}, Longhurst et al., 1995).

5.3.2 OMZ-related anoxic conditions

Redox-sensitive trace element concetrations (e.g., Mo and U) are widely used to decipher and reconstruct palaeoenvironmental conditions (Wignall, 1994; Tribovillard et al., 2006). The high Mo values in the LCMM mostly fluctuate between 25 and 100 ppm (Fig. 3) suggesting an anoxic environment with intermittently euxinic conditions (e.g., Scott and Lyons 2012). The subsequent abrupt increase in Mo values (> 100 ppm) in the UMM indicate a permanently euxinic condition with abundant dissolved Mo in the ocean, which suggests an unrestricted supply of Mo (Fig. 3). This is further confirmed by similar changes of the U and TS contents (Fig. 3). Therefore, permanently anoxic conditions (with transient euxinic episodes) dominated during deposition of the LCMM, whereas more intense conditions (euxinia) dominated during the deposition of the UMM.

5.3.3 Sediment inputs

Elements such as Al, K, Ti and Zr are rarely influenced by biogenic or diagenetic processes and have thus been widely used as detrital influx indicators (Tribovillard et al., 2006). The Gufeng Formation is characterized by low contents of these detrital-element proxies relative to the average upper continental crust (AUCC; McLennan, 2001) suggesting a distal environment and dilution with biogenic material. The strong, positive correlations between Al_2O_3 and K_2O, TiO_2, Zr (R^2 = 0.92, 0.86 and 0.54, respectively, Fig. 4c, d, e) supports their detrital origin and indicates a constant source area (e.g., Ross and Bustin, 2009). Systematic variations of these detrital-element proxies in the Gufeng Formation follows the chert-mudstone rhythms (Fig. 3), and reflects fluctuations of biogenic silica production and/or terrigenous flux, likely under the control of Milankovitch-scale orbital forcing (Yao et al., 2015).

5.3.4 Hydrodynamic conditions

The Zr/Al ratio can be used to indicate the intensity or persistence of bottom currents due to the enrichment of Zr in heavy mineral fractions which can be concentrated during winnowing (e.g., Dellwig et al., 2000; Böning et al., 2004, 2005). Higher Zr/Al ratios result from enrichment of the heavy, detrital mineral fraction at the expense of clay minerals (Böning et al., 2005). The Zr/Al ratios of the LCMM are variable, with high ratios in chert and low ratios in siliceous mudstone, whereas the ratios of the UMM are more stable and lower (Fig. 3). The higher Zr/Al ratios in the chert suggest more persistent bottom currents relative to the siliceous mudstone, thus we propose that the lithological variations may record different locations relative to an expanding and contracting OMZ (Fig. 14). Additionally, the extremely high Zr/Al values in the upper LCMM could include volcanic input from the Emeishan Large Igneous province.

5.3.5 The possible depositional model

During the Guadalupian, intense perennial upwelling developed with fluctuant primary productivity and anoxic/euxinic conditions dominated in the eastern Paleo-Tethys Margin of South China. During the deposition of the chert, transgression introduces abundant nutrients supply and results in enhanced thermohaline circulation, which further stimulates marine productivity and results in more ventilated OMZ (Fig. 14a). This high productivity resulted in a sufficient silica supply and OM to the sediments. However, the stronger bottom current activities and relatively weak reducing conditions could lead to the relatively poor preservation of organic matter and, thus, the relatively low TOC content in the chert. During the deposition of siliceous mudstone, regression associated with increased sediment inputs and intensified recycling of P maintained this high productivity. Enhanced heterotrophic respiration and subsequently subdued thermohaline circulation could have led to an expansion of the OMZ and, subsequently stronger reducing conditions (Fig. 14b). Combined with these weakened bottom current activities, as suggested by the less winnowed deposition within the ancient OMZ, both could have played a role in the preservation of OM and thus led to the higher TOC contents in the siliceous mudstone.

During the late Guadalupian, with the subdued upwelling activity and great regression, a rapid rise in the oceanic chemocline and diminished ocean circulation resulting from rapid global warming, which was triggered by the eruption of the Emeishan flood-basalt plateau in South China (e.g., Zhou et al., 2002; Wignall et al., 2009), may have led to a well-stratified water column and subsequently decreased oxygen exchange between the different water masses. During the deposition of the UMM, coupled with higher primary productivity (Fig. 14c), the intensified euxinic condition caused by a decreased oxygen exchange between the different water masses

411 further slowed down the decay of the labile organic-matter and favoured their enhanced

412 preservation in deeper water sediments and, thus, the highest TOC content.

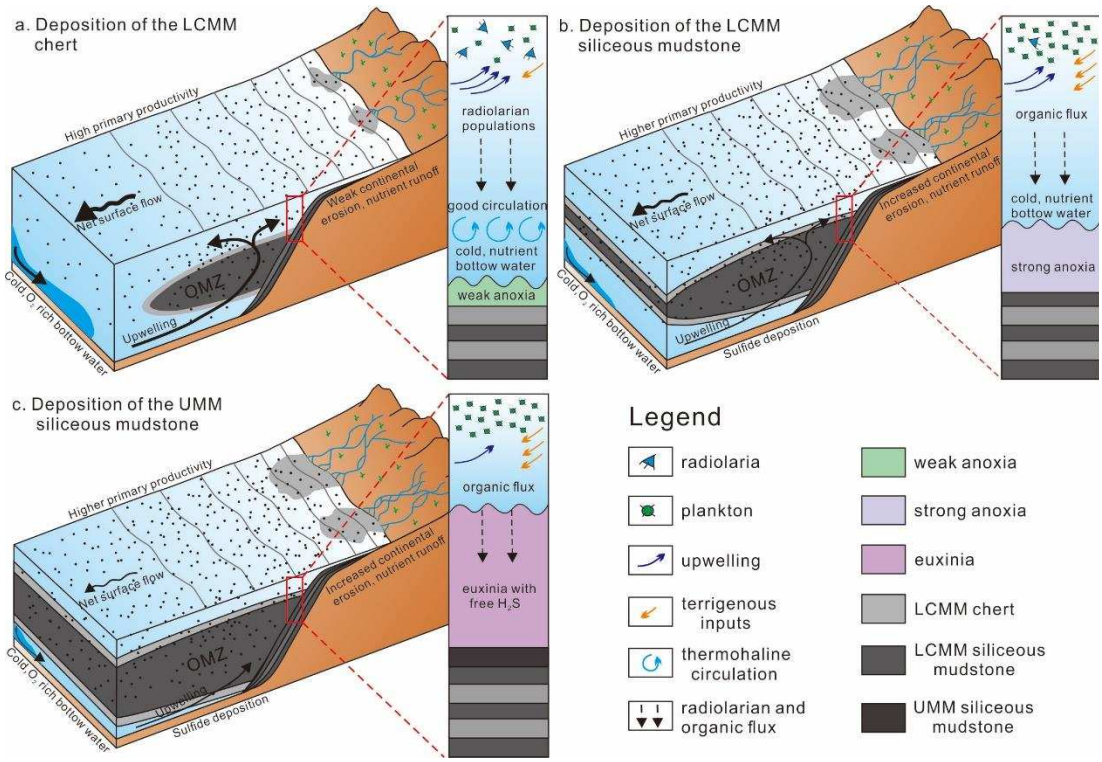

Fig. 14 A coastal upwelling model for the deposition of the Gufeng Formation along the eastern Paleo-Tethys Margin showing locations, relative to the OMZ, for the three main lithotypes (modified from Schoepfer et al., 2013).

413 5.4 Implications for the organic matter accumulation

414 Generally, coastal upwelling settings have high primary productivity resulting from the

415 enhanced nutrient supply from deep waters (Böning et al., 2004, 2015; Brongersma-Sanders et al.,

416 1980; Robinson et al., 2002; Scholz et al., 2011). The estimated palaeo-productivity of the Gufeng

417 Formation indicates similar primary productivity levels to those seen in modern upwelling setting,

418 which led to sufficient or even excess OM to transfer to the bottom water. The good correlation

419 between TOC and Ni also suggests that the OM influx increased with the enhanced primary

420 productivity (Fig. 13), which indicates that primary productivity could have direct controls on OM

421 accumulation. Although this high upwelling-driven primary productivity persisted, anoxic/euxinic

422 conditions occurred in the upwelling OMZ could also contribute to the burial and preservation of
423 OM and thus the high TOC content (e.g., Böning et al., 2004, 2015; Brongersma-Sanders et al.,
424 1980; Robinson et al., 2002; Scholz et al., 2011). However, the use of the Sweere et al. (2016)
425 discrimination diagram for tracking the relative importance of productivity versus preservation
426 shows that the Gufeng OM-enriched sediments fall in the productivity-controlled upwelling sector
427 (Fig. 15). Therefore, this upwelling-driven high primary productivity plays a major role in organic
428 matter accumulation.

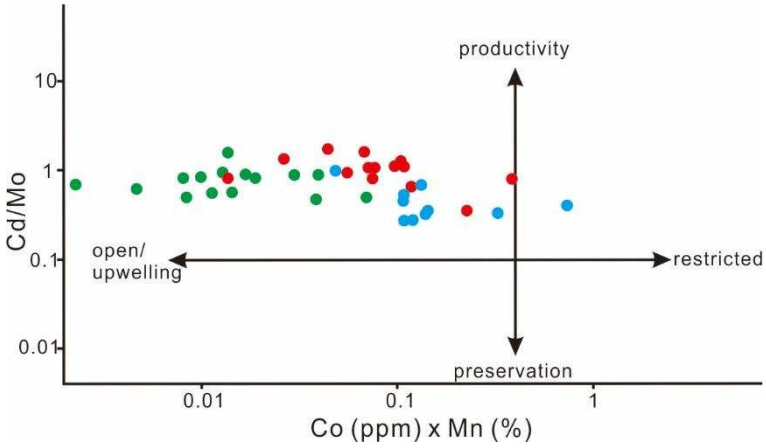

Fig. 15 Scatter plots of Co x Mn vs. Cd/Mo showing samples from the Gufeng Formation plot in the modern field for upwelling/high productivity (from Sweere et al., 2016).

429 Changes of sediment input have also been shown to influence organic matter accumulation
430 by dilution or adsorption (Sageman et al., 2003; Lash and Blood, 2014; Zeng et al., 2015). As
431 shown in figure 16, the relationship between the TOC and terrigenous elements is complex. The
432 positive correlations of detrital proxies (e.g., Al) and TOC (R^2 = 0.69, Fig. 16a) in the Gufeng
433 Formation suggests that both are controlled by dilution with biogenic silica (Fig. 4a, 16b). In
434 addition, clay minerals provided sites for organic matter adsorption on the aluminosilicates which
435 can aid preservation of OM (Kennedy et al., 2002).

436 Sediment transport and reworking by strong bottom currents must exert a major control on
437 OM preservation on the Peru Margin (Suess et al., 1987; Arthur, 1998). However, the weak

correlation between Zr/Al and TOC (R^2 = 0.13, Fig. 16c) in the Gufeng Formation indicates that bottom currents did not play a role in the preservation of OM. In addition, sediment bulk accumulation rates (Algeo et al., 2013; Tyson, 2005) may play an important role in the OM accumulation. However, the very weak correlation between TOC abundances and Ti/Al (R^2 = 0.08, Fig. 16d), which has been used as an indicator of sedimentation rate (e.g. Caplan and Bustin, 1999; Murphy et al., 2000), shows no consistent relationship between the organic matter concentrations and sedimentation rates.

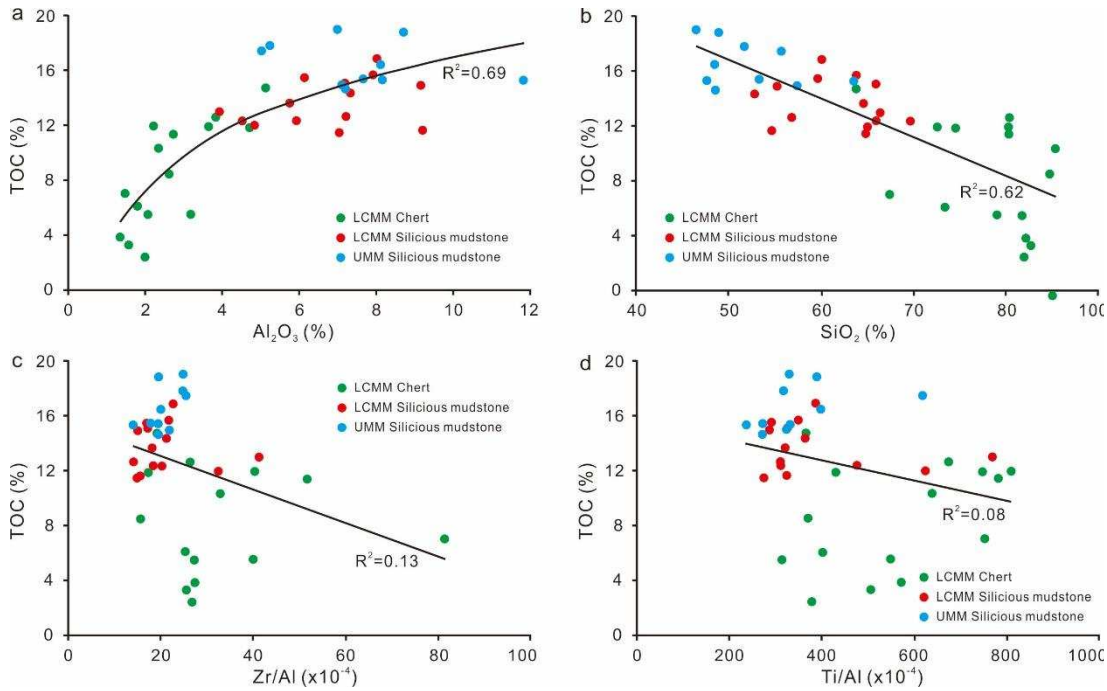

Fig. 16 Scatter plots of (a) Al_2O_3 vs. TOC, (b) SiO_2 vs. TOC, (c) Zr/Al vs. TOC, (d) Ti/Al vs. TOC.

6. Conclusion

Based on multiple geochemical indicators, we analysed the ancient upwelling system, reconstructed its palaeo-environmental conditions, and further improved our understanding of the controlling factors of organic matter accumulation. The following new results were obtained:

1. High organic carbon contents, similar enrichments of bio/redox-sensitive trace metals and bulk sedimentary composition, high Cd/Mo ratios and low Co x Mn values, which all show strong

similarities to the geochemical characteristics of modern upwelling sediments, implied that the Lower Yangtze region was dominated by persistent upwelling that become less intense (seasonal?) later in the Guadalupian.

2. This ancient coastal upwelling setting was characterized by moderate to high levels primary productivity, permanently anoxic conditions (with transient euxinic episodes), systematic sediment inputs and fluctuant bottom current activities.

3. The exceptional organic enrichment of the Middle Permian Gufeng Formation is attributed to elevated primary productivity due to upwelling along the continental margin of South China, and changes of anoxic/euxinic conditions and dilution of biogenic silica may also plays a role in these organic matter accumulation.

Acknowledgments

This work was supported by the National Natural Science Foundation of China (Grant nos. U1663202, 41372127, 41172139 and 41690131) and the Science and Technology program of Land and Resources of Anhui Province (Grant nos. 2015-K-4).

References

Algeo, T.J., Henderson, C.M., Tong, J., Feng, Q., Yin, H., Tyson, R.V., 2013. Plankton and productivity during the Permian-Triassic boundary crisis: An analysis of organic carbon fluxes. Global and Planetary Change 105, 52-67.

Algeo, T.J., Ingall, E., 2007. Sedimentary C-org : P ratios, paleocean ventilation, and Phanerozoic atmospheric pO(2). Palaeogeography Palaeoclimatology Palaeoecology 256(3-4), 130-155

Arthur, M.A., Dean, W.E., Laarkamp, K., 1998. Organic carbon accumulation and preservation in surface sediments on the Peru margin. Chemical Geology 152, 273-286.

Baturin, G.N., Oreshkin, V.N., 1985. Behavior of cadmium in ocean-floor bone phosphate. Geochemistry International 22(2), 69-74.

Beauchamp, B., Baud, A., 2002. Growth and demise of Permian biogenic chert along northwest Pangea: evidence for end-Permian collapse of thermohaline circulation. Palaeogeography Palaeoclimatology Palaeoecology 184, 37-63.

Böning, P., Brumsack, H.J., Bottcher, M.E., Schnetger, B., Kriete, C., Kallmeyer, J., Borchers, S.L.,

2004. Geochemistry of Peruvian near surface sediments. Geochimica Et Cosmochimica Acta 68, 4429-4451.

Böning, P., Brumsack, H.-J., Schnetger, B., Grunwald, M., 2009. Trace element signatures of Chilean upwelling sediments at 36S. Marine Geology 259, 112–121.

Böning, P., Cuypers, S., Grunwald, M., Schnetger, B., Brumsack, H.J.,2005. Geochemical characteristics of Chilean upwelling sediments at 36S. Marine Geology 220, 1–21.

Böning, P., Shaw, T., Pahnke, K., Brumsack, H.J., 2015. Nickel as indicator of fresh organic matter in upwelling sediments. Geochimica Et Cosmochimica Acta 162, 99-108.

Borchers, S.L., Schnetger, B., Boning, P., Brumsack, H.J., 2005. Geochemical signatures of the Namibian diatom belt: Perennial upwelling and intermittent anoxia. Geochemistry Geophysics Geosystems 6 (6), Q06006.

Boyle, E.A., Sclater, F., Edmond, J.M., 1976. Marine geochemistry of Cadmium. Nature 263, 42-44.

Brongersma-sanders, M., Stephan, K.M., Kwee, T.G., Debruin, M., 1980. Distribution of minor elements in cores from the Southwest Africa shelf with notes on plankton and fish mortality. Marine Geology 37, 91-132.

Bruland, K.W., 1983. Trace elements in seawater. In: Riley, J.P., Chester, R. (Eds.), Chemical Oceanography. Academic Press, London, pp. 157–220.

Brumsack, H.J., 1989. Geochemistry of recent TOC-rich sediments form the Gulf of California and the Black Sea. Geologische Rundschau 78, 851-882.

Brumsack, H. J., 2006. The trace metal content of recent organic carbon-rich sediments: implications for Cretaceous black shale formation. Palaeogeography, Palaeoclimatology, Palaeoecology 232(2-4), 344-361.

Bureau of Geology and Mineral Resources of Anhui Province, 1989. Stratigtaphic record of Anhui Province. Anhui Science and Technology Publishing House, pp.18-23, 86-90. (in Chinese)

Calvert, S.E., Pedersen, T.F., 1993. Geochemistry of Recent oxic and anoxic sediments: Implications for the geological record. Marine Geology 113, 67-88.

Calvert, S.E., Price, N.B., 1983. Geochemistry of Namibian shelf sediments. In: Suess, E., Thiede, J. (Eds.), Coastal Upwelling; Its Sediment Record. Part A. Plenum Press, New York, pp. 337–375.

Canfield, D.E., 1989. Reactive iron in marine-sediments. Geochimica Et Cosmochimica Acta 53, 619-632.

Caplan, M.L., Bustin, R.M., 1999. Palaeoceanographic controls on geochemical characteristics of organic-rich Exshaw mudrocks: role of enhanced primary production. Organic Geochemistry 30, 161-188.

Dellwig, O., Hinrichs, J., Hild, A., Brumsack, H.J., 2000. Changing sedimentation in tidal flat sediments of the southern North Sea from the Holocene to the present: a geochemical approach. Journal of Sea Research 44, 195-208.

Demaison, G.J., Moore, G.T., 1980. Anoxic environments and oil source red genesis. AAPG Bulletin-American Association of Petroleum Geologists 64, 1179-1209.

Du, X., Song X., Zhang, M., Lu, Y., Chen, P., Liu, Z. Yang, S., 2015. Shale gas potential of the Lower Permian Gufeng Formation in the western area of the Lower Yangtze Platform, China. Marine and Petroleum Geology 67: 526-543.

Enkin, R.J., Yang, Z.Y., Chen, Y., Courtillot, V., 1992. Paleomagnetic constraints on the

geodynamic history of the major blocks of China from the Permian to the present. Journal of Geophysical Research-Solid Earth 97, 13953-13989.

Feng, Z., He, Y., Wu, S., 1993. Lithofacies paleogeography of Permian Middle and Lower Yangtze region. Acta Sedimentological Sinica 12-24 (in Chinese with English abstract)

Haraldsson, C., Westerlund, S., 1988. Trace-metals in the water columns of the Black Sea and Framvaren Fjord. Marine Chemistry 23, 417-424.

Heggie, D., Lewis, T., 1984. Cobalt in pore waters of marine sediments. Nature 311, 453-455.

Ho, T. Y., Quigg, A., Finkel, Z. V., Milligan, A. J., Wyman, K., Falkowski, P. G., Morel, F. M., 2003. The elemental composition of some marine phytoplankton. Journal of phycology 39(6): 1145-1159.

HO, T. Y. 2006. The trace metal composition of marine microalgae in cultures and natural assemblages, In D. V. Subba Rao [ed.], Algal cultures: Analogues of blooms and applications. Science Publishers, p. 271–299.

Ibach, L.E.J., 1982. Relationship between sedimentation rate and total organic carbon content in ancient marine sediments. Am. Assoc. Pet. Geol. Bull. 66, 170-188.

Ikeda, M., Tada, R., Ozaki, K., 2017. Astronomical pacing of the global silica cycle recorded in Mesozoic bedded cherts. Nature Communications 8.

Ingall, E., Jahnke, R., 1997. Influence of water-column anoxia on the elemental fractionation of carbon and phosphorus during sediment diagenesis. Marine Geology 139, 219-229.

Kametaka, M., Takebe, M., Nagai, H., Zhu, S., Takayanagi, Y., 2005. Sedimentary environments of the Middle Permian phosphorite-chert complex from the northeastern Yangtze platform, China; the Gufeng Formation: a continental shelf radiolarian chert. Sedimentary Geology 174, 197-222.

Kennedy, M. J., Pevear, D. R., Hill, R. J., 2002. Mineral surface control of organic carbon in black shale. Science 295(5555), 657-60.

Lawrence, C.R., Neff, J.C., 2009. The contemporary physical and chemical flux of aeolian dust: A synthesis of direct measurements of dust deposition. Chemical Geology 267, 46-63.

Lash, G.G., Blood, D.R., 2014. Organic matter accumulation, redox, and diagenetic history of the Marcellus formation, southwestern Pennsylvania, Appalachian basin. Mar. Pet. Geol. 57, 244–263.

Liang D., Guo, T., Bian, L., Chen, J., Zhao, Z., 2009. Some progresses on studies of hydrocarbon generation and accumulation in marine sedimentary regions, Southern China (Part 3) : controlling factors on the sedimentary facies and development of Palaeozoic marine source rocks. Marine origin petroleum geology 14, 1-19 (in Chinese with English abstract)

Little, S.H., Vance, D., Lyons, T.W., McManus, J., 2015. Controls on trace metal authigenic enrichment in reducing sediments: insights from modern oxygen-deficient settings. American Journal of Science, 315(2), 77-119

Longhurst, A., Sathyendranath, S., Platt, T., Caverhill, C., 1995. An estimate of global primary production in the ocean from satellite radiometer data. Journal of Plankton Research 17, 1245-1271.

Lv, B., Qu, J., 1989. The Early Permian anoxic deposits from transgression and uplifting flow in the Lower Yangtze region. Chinese Science Bulletin 34, 1721-1724 (in Chinese)

Lyons, T.W., Berner, R.A., 1992. Carbon sulfur iron systematics of the uppermost deep-water sediments of the Black Sea. Chemical Geology 99, 1-27.

Lyons, T.W., Werne, J.P., Hollander, D.J., Murray, R.W., 2003. Contrasting sulfur geochemistry and Fe/Al and Mo/Al ratios across the last oxic-to-anoxic transition in the Cariaco Basin, Venezuela.

Chemical Geology 195, 131-157.

McLennan, S.M., 2001. Relationships between the trace element composition of sedimentary rocks and upper continental crust. Geochemistry Geophysics Geosystems, 2.

Moore, C. M., Mills, M. M., Arrigo, K. R., Berman-Frank, I., Bopp, L., Boyd, P. W., Galbraith, E. D., Geider, R. J., Guieu, C., Jaccard, S. L., Jickells, T. D., La Roche, J., Lenton, T. M., Mahowald, N. M., Marañón, E., Marinov, I., Moore, J. K., Nakatsuka, T., Oschlies, A., Saito, M. A., Thingstad, T. F., Tsuda, A., Ulloa, O., 2013. Processes and patterns of oceanic nutrient limitation. Nature Geoscience 6(9), 701.

Morse, J.W., Luther, G.W., 1999. Chemical influences on trace metal-sulfide interactions in anoxic sediments. Geochimica Et Cosmochimica Acta 63, 3373-3378.

Murchey, B.L., Jones, D.L., 1992. A mid-Permian chert event – widespread deposition of biogenic siliceous sediments in coastal, island-arc and oceanic basins. Palaeogeography Palaeoclimatology Palaeoecology 96, 161-174.

Murphy, A. E., Sageman, B. B., Hollander, D. J., Lyons, T. W., Brett, C. E., 2000. Black shale deposition and faunal overturn in the Devonian Appalachian Basin: Clastic starvation, seasonal water-column mixing, and efficient biolimiting nutrient recycling. Paleoceanography 15(3), 280-291.

Nathan, Y., Soudry, D., Levy, Y., Shitrit, D., Dorfman, E., 1997. Geochemistry of Cadmium in the Negev phosphorites. Chemical Geology 142, 87-107.

Parrish, J.T., 1982. Upwelling and petroleum source beds, with reference to Paleozoic. AAPG Bulletin-American Association of Petroleum Geologists 66, 750-774.

Parrish, J.T., Curtis, R.L., 1982. Atmospheric circulation, upwelling, and organic-rich rocks in the Mesozoic and Cenozoic eras. Palaeogeography Palaeoclimatology Palaeoecology 40, 31-66.

Pedersen, T.F., Calvert, S.E., 1990. Anoxia VS productivity – what controls the formation of organic-carbon-rich sediments and sedimentary-rocks. AAPG Bulletin-American Association of Petroleum Geologists 74, 454-466.

Robinson, R.S., Meyers, P.A., Murray, R.W., 2002. Geochemical evidence for variations in delivery and deposition of sediment in Pleistocene light-dark color cycles under the Benguela Current Upwelling System. Marine Geology 180, 249-270.

Rollison, H., 1993. Using Geochemical Data. Longman, Harlow, pp. 352.

Ross, D.J.K., Bustin, R.M., 2009. Investigating the use of sedimentary geochemical proxies for paleoenvironment interpretation of thermally mature organic-rich strata: Examples from the Devonian-Mississippian shales, Western Canadian Sedimentary Basin. Chemical Geology 260, 1-19.

Sageman, B.B., Murphy, A.E., Werne, J.P., Straeten, C.A.V., Hollander, D.J., Lyons, T.W., 2003. A tale of shales: the relative roles of production, decomposition, and dilution in the accumulation of organic-rich strata, Middle–Upper Devonian, Appalachian basin. Chemical Geology 195, 229-273.

Saitoh, M., Isozaki, Y., Yao, J., Ji, Z., Ueno, Y., Yoshida, N., 2013. The appearance of an oxygen-depleted condition on the Capitanian disphotic slope/basin in South China: Middle-Upper Permian stratigraphy at Chaotian in northern Sichuan. Global and Planetary Change 105, 180-192.

Schoepfer, S.D., Henderson, C.M., Garrison, G.H., Foriel, J., Ward, P.D., Selby, D., Hower, J.C., Algeo, T.J., Shen, Y., 2013. Termination of a continent-margin upwelling system at the Permian-Triassic boundary (Opal Creek, Alberta, Canada). Global Planet. Change 105, 21–35.

Schoepfer, S.D., Shen, J., Wei, H., Tyson, R.V., Ingall, E., Algeo, T.J., 2015. Total organic carbon, organic phosphorus, and biogenic barium fluxes as proxies for paleomarine productivity. Earth-

612 Science Reviews 149, 23-52.
613 Scholz, F., Hensen, C., Noffke, A., Rohde, A., Liebetrau, V., Wallmann, K., 2011. Early diagenesis
614 of redox-sensitive trace metals in the Peru upwelling area - response to ENSO-related oxygen
615 fluctuations in the water column. Geochimica Et Cosmochimica Acta 75, 7257-7276.
616 Scott, C., Lyons, T.W., 2012. Contrasting molybdenum cycling and isotopic properties in euxinic
617 versus non-euxinic sediments and sedimentary rocks: Refining the paleoproxies. Chemical Geology
618 324, 19-27.
619 Scott, C., Slack, J. F., Kelley, K. D, 2017. The hyper-enrichment of V and Zn in black shales of
620 the Late Devonian-Early Mississippian Bakken Formation (USA). Chemical Geology 452, 24-33.
621 Shen, J., Schoepfer, S.D., Feng, Q., Zhou, L., Yu, J., Song, H., Wei, H., Algeo, T.J., 2015. Marine
622 productivity changes during the end-Permian crisis and Early Triassic recovery. Earth-Science
623 Reviews 149, 136-162.
624 Shi, L., Feng, Q., Shen, J., Ito, T., Chen, Z.Q., 2016. Proliferation of shallow-water radiolarians
625 coinciding with enhanced oceanic productivity in reducing conditions during the Middle Permian,
626 South China: evidence from the Gufeng Formation of western Hubei Province. Palaeogeography
627 Palaeoclimatology Palaeoecology 444, 1-14.
628 Suess, E., Kulm, L. D., Killingley, J. S., 1987. Coastal upwelling and a history of organic rich
629 mudstone deposition off Peru. Geological Society London Special Publications 26 (1), 181 – 197.
630 Sweere, T., van den Boorn, S., Dickson, A.J., Reichart, G.J., 2016. Definition of new trace-metal
631 proxies for the controls on organic matter enrichment in marine sediments based on Mn, Co, Mo
632 and Cd concentrations. Chemical Geology 441, 235-245.
633 Tribovillard, N., Algeo, T.J., Lyons, T., Riboulleau, A., 2006. Trace metals as paleoredox and
634 paleoproductivity proxies: An update. Chemical Geology 232, 12-32.
635 Tyson, R.V., 2005. The “productivity versus preservation” controversy: cause, flaws, and
636 resolution. In: Harris, N.B. (Ed.), Deposition of Organic-Carbon-Rich Sediments: Models,
637 Mechanisms, and Consequences. Society for Sedimentary Geology (SEPMSSG) Special Publication
638 82, pp. 17–33.
639 Van der Weijden, C. H., 2002. Pitfalls of normalization of marine geochemical data using a
640 common divisor. Marine Geology 184(3-4), 167-187.
641 Wang, J., Jin, Y.G., 2000. Permian palaeogeographic evolution of the Jiangnan Basin, South
642 China. Palaeogeography Palaeoclimatology Palaeoecology 160(1-2), 35-44.
643 Wang, R., Shen, G., Katsuo, S., 1997. Studies on radiolarian fauna from Gufeng Formation in
644 Anhui and Jiangsu provinces, East China and its paleoenvironmental significance. Journal of Tongji
645 University 25(5), 559-564 (in Chinese with English abstract)
646 Wedepohl, K.H., 1991. The composition of the upper earth's crust and the natural cycles of
647 selected metals. Metals in natural raw materials. Natural Resources. In: Merian, E. (Ed.), Metals
648 and their compounds in the environment. VCH, Weinheim, pp. 3–17.
649 Wignall, P.B. 1994. Black shales. Oxford University Press, Oxford, pp. 130.
650 Wignall, P.B., Sun, Y., Bond, D.P.G., Izon, G., Newton, R.J., Vedrine, S., Widdowson, M., Ali, J.R.,
651 Lai, X., Jiang, H., Cope, H. and Bottrell, S.H., 2009. Volcanism, Mass Extinction, and Carbon Isotope
652 Fluctuations in the Middle Permian of China. Science, 324(5931), 1179-1182.
653 Wu, K., Ma, Q., Feng, Q., 2015. Stratigraphic division and spatial distribution of the Middle
654 Permian Kuhfeng Formation in the northern Yangtze block. Journal of Stratigraphy 39(1), 33-39. (in
655 Chinese with English abstract)

Xu, W., 1990. On the origins of the Permian siliceous rocks in Jiangsu-Zhejiang-Anhui provinces and their relation with the generation of oil and gas. Experimental petroleum geology 12(1), 44-48 (in Chinese with English abstract)

Yao, X., Zhou, Y., Hinnov, L.A., 2015. Astronomical forcing of a Middle Permian chert sequence in Chaohu, South China. Earth and Planetary Science Letters 422, 206-221.

Zeng, S.Q., Wang, J., Fu, X.G., Chen, W.B., Feng, X.I., Wang, D., Song, C.Y., Wang, Z.W., 2015. Geochemical characteristics, redox conditions, and organic matter accumulation of marine oil shale from the Changliang Mountain area, northern Tibet, China. Mar. Pet. Geol. 64, 203–221.

Zhou, M., Malpas, J., Song, X., Robinson, P.T., Sun, M., Kennedy, A.K., Lesher, C.M. and Keays, R.R., 2002. A temporal link between the Emeishan large igneous province (SW China) and the end-Guadalupian mass extinction. Earth and Planetary Science Letters, 196(3-4), 113-122.